Tritium transport model at the minimal functional unit level for HCLL and WCLL breeding blankets of DEMO

Tritium transport model at the minimal functional unit level for HCLL and WCLL breeding blankets of DEMO

Luigi Candido[a], Raffaella Testoni[a], Marco Utili[b], Massimo Zucchetti[a]

[a]*Dipartimento Energia, Politecnico di Torino, Corso Duca degli Abruzzi 24 – Torino, Italy*
[b]*ENEA UTIS-C.R. Brasimone, Bacino del Brasimone, Camugnano, BO, Italy*

The Helium-Cooled Lithium-Lead (HCLL) and Water-Cooled Lithium-Lead (WCLL) Breeding Blankets are two of the four European blanket designs proposed for DEMO reactor. A tritium transport model inside the blankets is fundamental to assess their preliminary design and safety features. Tritium transport and permeation are complex phenomena to be taken into account in the evaluation of tritium balance in order to guarantee tritium self-sufficiency and to characterise tritium concentrations, inventories and losses. In this context, the study has been performed at the minimal functioning unit level of the outboard equatorial breeding blanket module, which is, during continuous operative conditions, one of the most loaded modules and this results in higher permeation phenomena. For these purposes, a 2D model for the breeder unit of HCLL and a 3D model for the single cell of WCLL breeding blanket concepts have been investigated. The model includes advection-diffusion of tritium into the lead-lithium eutectic alloy, transfer of tritium from the liquid interface towards the steel, diffusion of tritium inside the steel, transfer of tritium from the steel towards the coolant, and advection-diffusion of diatomic tritium into the coolant. Temperature fields, tritium generation rate profiles, velocity profile of lead-lithium have been also taken into account.

Keywords: tritium transport, breeding blanket, HCLL, WCLL, DEMO

1. Introduction

In fusion reactors, the prediction of tritium transport in lead-lithium liquid metal blankets and the quantification of permeation rate from the lead-lithium liquid metal breeder into the helium coolant are fundamental [1]. Tritium transport and permeation are important in order to guarantee tritium self-sufficiency and to characterize tritium concentrations, inventories and losses. One of the goals is to control tritium permeation towards cooling system to an acceptable level [2] since tritium could reach the environment, representing a potential radiological risk [3]. The major issues related to the development of a tritium transport model under fusion-relevant conditions are due to its multi-physics, multi-material domains, and complex blanket geometry. Since a large number of variables that affects the tritium behaviour have to be considered simultaneously, a comprehensive model has not yet been fully developed. However, in literature it is possible to find some tritium transport models [2, 4-10].

Four European breeding blankets designs have been proposed for DEMO reactor [11]. In this study, the Helium-Cooled Lithium-Lead (HCLL) and Water-Cooled Lithium-Lead (WCLL) have been considered. The aim of this work is to study the minimal functional unit in the outboard equatorial module: breeder unit for HCLL, and single cell for WCLL. Hence, two transport models have been implemented, taking into account transport and interface phenomena, temperature fields, tritium generation rate profiles, and Pb-15.7Li velocity profiles. Tritium concentrations, inventories and losses have been estimated by means of Comsol Multiphysics 5.3.

2. Description of the model

2.1 General overview of the transport model

A scheme of tritium transport phenomena which occur in HCLL and WCLL breeding blankets is shown in Fig. 1. It is possible to identify the processes taken into account: a) advection-diffusion of tritium into the lead-lithium eutectic alloy; b) diffusion of tritium inside the steel; c) advection-diffusion of diatomic tritium into the coolant; d) transfer of tritium from the liquid interface towards the Eurofer (adsorption/desorption); e) transfer of tritium from the solid interface towards the coolant (recombination/desorption).

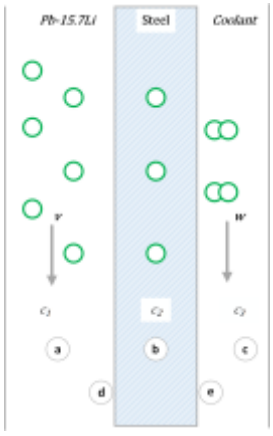

Fig. 1. Simplified scheme of the transport process.

It has to be pointed out that only tritium is considered for the present analysis. We neglect the formation of HT and HTO species because no ancillary systems have been considered and no chemistry control is taken into account.

2.2 Governing equations

author's email: luigi.candido@polito.it

Referring to **Error! Reference source not found.**, tritium transport in the domains (a), (b) and (c) can be described by a scalar partial differential equation which includes the diffusion and the advection contribution:

$$\frac{\partial c_i}{\partial t} + \nabla \cdot \vec{\mathbf{u}} c_i - \nabla \cdot (D_i \nabla c_i) = s \qquad (1)$$

where c_i [mol · m^{-3}] is the tritium concentration in the i-th domain (lead-lithium, Eurofer, coolant), $\vec{\mathbf{u}}$ [m · s^{-1}] is the velocity field, D_i [m^2 · s^{-1}] is the diffusion coefficient of tritium and s [mol · m^{-3} · s^{-1}] is the molar tritium generation rate along the radial coordinate. For the steels, e.g. cooling plates or horizontal stiffening plates, there is no tritium source and the process is governed by pure diffusion of tritium through the structures, whereas in the coolant tritium transport is governed by both advection and diffusion and no sources are present.

At the interface between lead-lithium and steel (d), the continuity of the partial pressure of tritium has been imposed:

$$c_1 = c_2 \cdot K_{1,2} \qquad (2)$$

where $K_{1,2}$ is the partition coefficient, defined as the ratio between the Sieverts' constant of the liquid metal and the one of the steel. At the steel/coolant interface (e), a flux discontinuity for the tritium in Eurofer and for the tritium in the coolant is imposed:

$$\phi_{2,3} = -2k_r \cdot c_2^2 \qquad (3)$$

$$\phi_{3,3} = -k_d \cdot \left(\frac{c_3}{k_H}\right) \cdot \delta + 2k_r \cdot c_2^2 \qquad (4)$$

where k_r and k_d are the recombination and dissociation coefficient, respectively, k_H in the Henry's constant of solubility and δ is equal to 1 in case of WCLL single cell and 0 in case of HCLL breeder unit.

The velocity and pressure fields can be derived by the Navier-Stokes equations of momentum and mass conservation; moreover, the velocity appears in the conduction-convection heat equation. The resulting set of four partial differential equations is completed by a specific model for the turbulence of the coolant. In order to achieve a relatively fast convergence of the solution, the $k-\varepsilon$ model has been chosen, where k [m^2 · s^{-2}] represents the turbulent kinetic energy and ε [m^2 · s^{-3}] is the turbulent dissipation rate. The complete set of PDEs is reported in [12].

2.3 Inventories and losses

Two main derived data are tritium inventory and tritium losses. Tritium inventory is evaluated by means of the following equation:

$$\mathrm{I}_i(t) = M_T \cdot \tau \cdot \int_{\Omega_i} C_i(\vec{x}, t) \cdot d\vec{x} \qquad (5)$$

where M_T is the atomic/molecular weight of tritium, τ is equal to the toroidal length of the minimal functional unit in HCLL and 1 in WCLL, Ω_i is the radial-poloidal area of the *i*-th domain (lead-lithium, Eurofer, coolant) for HCLL and the volume of the *i*-th domain for WCLL and C_i is the concentration.

Tritium losses are evaluated through the equation:

$$\Phi_{\text{losses}}(t) = M_T \cdot \iint_{\Omega_{coolant}} \phi_{leak}(\vec{x}, t) \cdot d\vec{x} \qquad (6)$$

where ϕ_{leak}[mol · m^{-2} · s^{-1}] is the total flux which goes out from the coolant domain, and $\Omega_{coolant}$ is the interfacial area between Eurofer and coolant.

3. Input data

3.1 HCLL breeder unit

The optimised-conservative design [13] is considered, for which the HCLL breeder unit geometry is characterized by 3 manifold, two horizontal stiffening plates (hSPs), two vertical stiffening plates (vSPs) and two cooling plates (CPs). The model has been developed in 2D geometry, considering only half of the full geometry shown in Fig. 2, in order to reduce, as much as possible, the computational time.

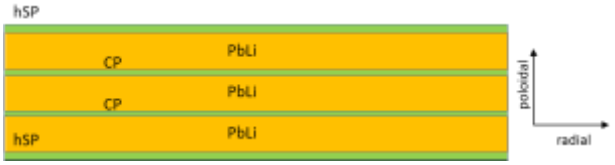

Fig. 2. Optimised-conservative design of the breeder unit.

Thermal-hydraulics calculations have been carried out considering both the uniform thermal heat flux at the first wall and the exponential radial volumetric heat generation rate. The thermal heat flux has been used in a 3D model of the first wall, in order to calculate the lead-lithium inlet temperature in the breeder unit. To investigate the suitable boundary conditions in terms of inlet temperatures and velocities, a 2D model of the stiffening plates and cooling plates has been implemented. From these thermal fields, the calculation of tritium transport in the breeder unit has been performed assuming the boundary conditions used to fulfil the design criteria reported in [13]. The model takes into considerations the viscous dissipation and the work done by the pressure. The main input data are reported in Table 1. Materials properties for the Pb-15.7Li, Eurofer and helium, as well as the tritium generation rate G [mol m^{-3}s^{-1}] and the volumetric heat generation rates $\dot{Q}$ [W m^{-3}], are taken from [14-16]. The diffusion coefficient of tritium into helium has been evaluated by means of the theoretical model developed by Chapman and Enskog [17]. Reiter's correlation for Sieverts' constant of tritium solubility into lead-lithium has been adopted [18].

Table 1. Main input data for the HCLL breeder unit.

Boundary type	Value	Description
$T_{in,LM}$	331 [°C]	Lead-lithium inlet temperature
p_{LM}	5 [bar]	Lead-lithium inlet pressure
v_{LM}	2.5 [mm/s]	Lead-lithium inlet velocity
Φ_{sup}	0.5 [MW/m^2]	Thermal heat flux on the first wall
$v_{He,CP}$	70 [m/s]	Helium inlet velocity into CPs
$v_{He,hSP}$	50 [m/s]	Helium inlet velocity into hSPs
p_{He}	80 [bar]	Helium inlet pressure

3.2 WCLL single cell

The WCLL single cell is one of the 16 elementary cells constituting the equatorial outboard module box

[19]. Divided in the middle by a baffle plate, in each elementary cell the PbLi enters from the bottom, flows in radial-poloidal direction and exits from the top. Since water is in cross-flow with respect to the lead-lithium eutectic alloy, tritium transport is modelled in radial-poloidal-toroidal direction. In Fig. 3, a scheme of WCLL outboard module radial-poloidal cut view is shown.

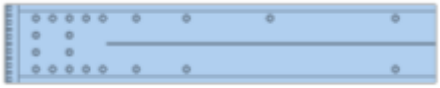

Fig. 3. Radial-poloidal cut view of WCLL single cell.

As a first approach for the WCLL single cell, the thermal fields variables have not been coupled to the Navier-Stokes' equations and to the tritium transport equation. The mean temperatures evaluated by solving the conduction-convection heat equation have been used to evaluated the transport parameters. Eurofer and lead-lithium properties are the same as HCLL; diffusion coefficient and Henry's constant of solubility of tritium in water have been derived from the correlations by Wilke-Chang [20] and Harvey [21], respectively. Due to a lack of information related to the tritium generation rate inside the single cell, as a first attempt the HCLL tritium generation rate has been assumed. The volumetric heat generation rate has been taken from [19]. Reiter's correlation for Sieverts' constant has been adopted. The main input data are reported in Table 2.

Table 2. Main input data for the WCLL single cell.

Boundary type	Value	Description
$T_{in,LM}$	325 [°C]	Lead-lithium inlet temperature
p_{LM}	5 [bar]	Lead-lithium inlet pressure
v_{LM}	1 [mm/s]	Lead-lithium inlet velocity
Φ_{sup}	0.5 [MW/m^2]	Thermal heat flux on the first wall
$T_{in,w}$	285 [°C]	Water inlet temperature
$v_{w,FW}$	1.24 [m/s]	Water inlet velocity in FW
$v_{w,BZ}$	1.57 [m/s]	Water inlet velocity in BZ
p_w	155 [bar]	Water inlet pressure

4. Results

4.1 HCLL BU results

The average concentrations in the different materials involved in the calculations are shown in the following graphs. A simulation time of 120 minutes has been performed to identify the equilibrium condition of concentrations, inventories and losses. Tritium concentration inside the Pb-15.7Li is reported in Fig. 4.

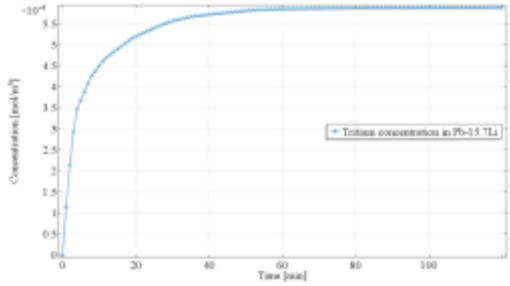

Fig. 4. Tritium concentration into lead-lithium.

Concerning the Eurofer cooling plates and stiffening plates, their average tritium concentration is reported in Fig. 5. The average tritium concentration in helium is shown in Fig. 6. It can be noticed that, in absence of a chemistry control, the value of diatomic tritium concentration is very low if compared to the concentration into lead-lithium and Eurofer. These results confirm the choice to neglect the diatomic tritium concentration in similar works [2, 4-10].

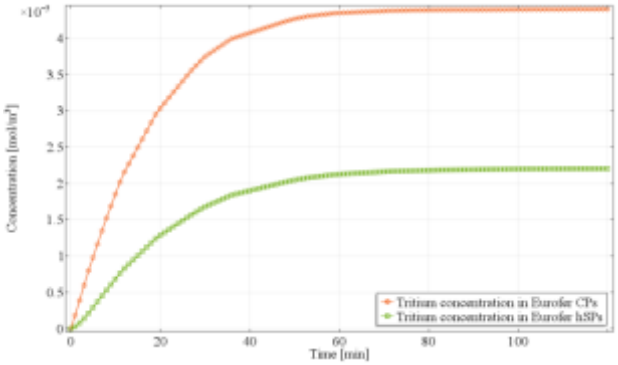

Fig. 5. Tritium concentration into Eurofer CPs and hSPs.

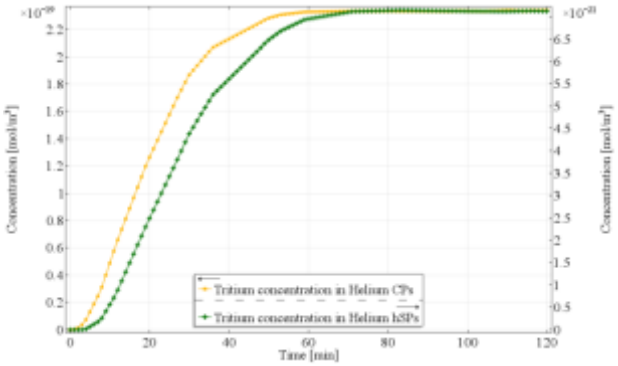

Fig. 6. Tritium concentration into helium coolant.

In Table 3 a resume of the previous calculation in terms of equilibrium concentrations and time needed to reach 99% of equilibrium (t^*) is reported.

Table 3. Concentrations and times to reach equilibrium for HCLL breeder unit.

Concentration	Equilibrium conc. [mol/m^3]	t^* [min]
T in Pb-15.7Li	$5.88 \cdot 10^{-4}$	52
T in Eurofer (CPs)	$4.40 \cdot 10^{-5}$	63
T in Eurofer (hSPs)	$2.21 \cdot 10^{-5}$	80
T_2 in Helium (CPs)	$2.34 \cdot 10^{-19}$	56
T_2 in Helium (hSPs)	$7.10 \cdot 10^{-21}$	67

Starting from the obtained concentrations, the inventories in Pb-15.7Li, Eurofer and helium have been estimated through equations (4) and (5). It must be pointed out that tritium is in atomic form in lead-lithium and Eurofer, whilst is diatomic in helium: this has been taken into account in the evaluation of inventories and losses. Without any H_2/H_2O addition into the coolant system, the amount of tritium permeating into the helium inside the breeder unit is very small if compared to the inventory in Pb-15.7Li and is in the order of 10^{-15} μg.

A resume of inventories and losses is given in

Table **4** and

Table **5**.

Table 4. Inventories in HCLL breeder unit.

Inventories	Equilibrium inv. [μg]
T in Pb-15.7Li	28.10
T in Eurofer (CPs)	$5.42 \cdot 10^{-2}$
T in Eurofer (hSPs)	$1.09 \cdot 10^{-1}$
T in Eurofer (total)	0.16
T_2 in Helium (CPs)	$1.30 \cdot 10^{-15}$
T_2 in Helium (hSPs)	$5.30 \cdot 10^{-17}$
T_2 in Helium (total)	$1.35 \cdot 10^{-15}$

Table 5. Tritium losses for HCLL breeder unit.

Material	T_2 losses [g/y]	T_2 losses [Ci/d]
T_2 in Helium (CPs)	$2.76 \cdot 10^{-11}$	$7.22 \cdot 10^{-10}$
T_2 in Helium (hSPs)	$8.64 \cdot 10^{-10}$	$2.26 \cdot 10^{-13}$

4.2 WCLL BU results

The average concentrations in the different materials involved in the calculations are shown in the following graphs. A simulation time of 480 minutes has been performed to identify the equilibrium state condition of concentrations, inventories and losses. Tritium concentration inside the Pb-15.7Li is reported in Fig. 7 for 120 minutes of the simulation. Tritium concentration in pipes, baffle and hSPs is shown in Fig. 7. The average tritium concentration in water for each poloidal column of pipes from FW to Pb-15.7Li inlet/outlet is shown in Fig. 9.

In Table 6**, a resume of the previous calculation in terms of equilibrium concentrations and time needed to reach 99% of equilibrium (t^*) is reported. A resume of inventories and losses is given in**

Table 7 and Table 8.

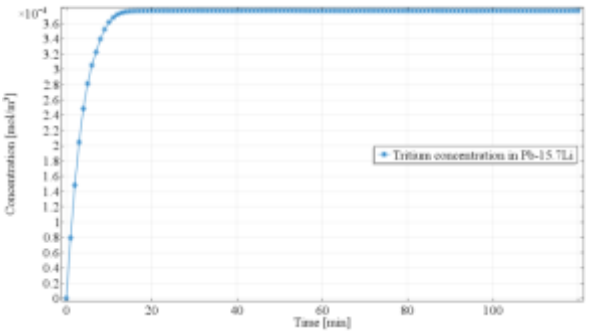

Fig. 7. Tritium concentration into lead-lithium.

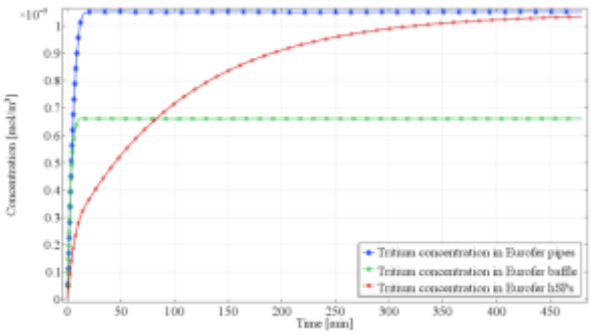

Fig. 8. Tritium concentration into Eurofer pipes, baffle and hSPs.

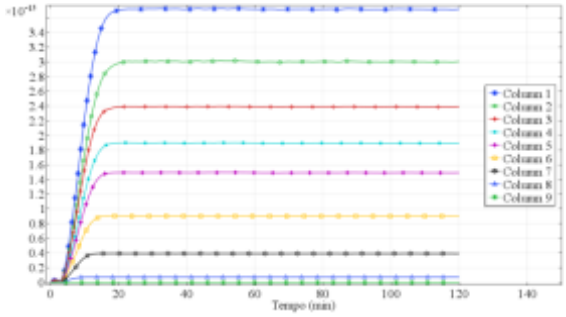

Fig. 9. Tritium concentration into water for each poloidal column of pipes from FW to Pb15.7Li inlet/outlet.

Table 6. Concentrations and times to reach equilibrium for WCLL breeder unit.

Concentration	Equilibrium conc. [mol/m^3]	t^* [min]
T in Pb-15.7Li	$3.73 \cdot 10^{-4}$	12
T in Eurofer (pipes)	$1.04 \cdot 10^{-5}$	15
T in Eurofer (baffle)	$5.57 \cdot 10^{-6}$	5
T in Eurofer (hSPs)	$1.03 \cdot 10^{-5}$	406
T_2 in Water	$1.88 \cdot 10^{-15}$	18

Table 7. Inventories in WCLL single cell.

Inventories	Equilibrium inv. [μg]
T in Pb-15.7Li	24.7
T in Eurofer (pipes)	$1.37 \cdot 10^{-2}$
T in Eurofer (baffle)	$5.82 \cdot 10^{-3}$
T in Eurofer (hSPs)	$1.38 \cdot 10^{-1}$
T in Eurofer (total)	0.16
T_2 in Water (total)	$2.68 \cdot 10^{-12}$

Table 8. Tritium losses for WCLL single cell.

Material	T_2 losses [g/y]	T_2 losses [Ci/d]
T_2 in Water	$1.50 \cdot 10^{-6}$	$3.97 \cdot 10^{-5}$

5. Discussion of the results

The comparison of tritium inventory in the lead-lithium, Eurofer and coolant in the HCLL breeder unit and in the WCLL single cell is shown in Fig. 10.

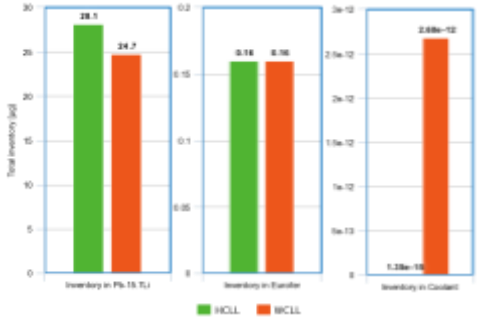

Fig. 10. Comparison between HCLL and WCLL inventories

HCLL inventory is 12% higher than WCLL, whereas in Eurofer the inventory is the same. As regards the coolant, the inventory in the water is about 2000 higher than in helium. This discrepancy can be searched in the difference of three order of magnitude in the diffusion coefficient of tritium in helium and of diffusion coefficient of tritium in water. Tritium inventory in Eurofer is shown in Fig. 11. For Both HCLL and WCLL concepts, most of tritium is stored inside the hSPs (68% and 86%, respectively).

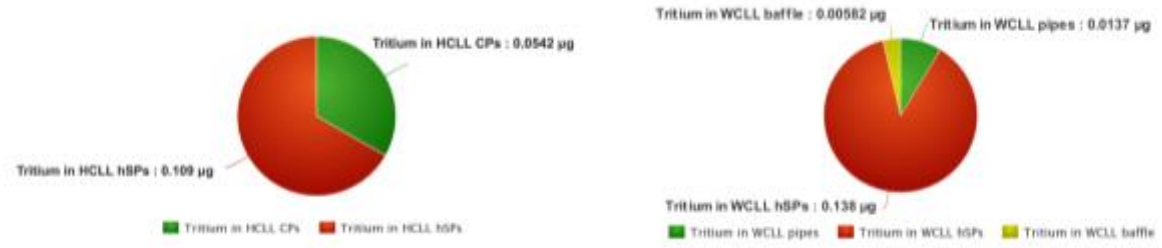

Fig. 11. Comparison between HCLL and WCLL inventories in Eurofer

Concerning the losses of tritium into the coolant, the HCLL has losses which can be neglected with respect to the WCLL, which has tritium losses about 50000 times higher with respect to the HCLL.

The time needed to reach the equilibrium is strongly influenced by the lead-lithium velocity field. In the HCLL the velocity profile is smooth, whereas in the WCLL there are zones where the velocity is almost null. This influences the transport process: in fact, in the proximity of the baffle and of Eurofer pipes the velocity reaches the maximum values, whereas near the hSPs it is almost zero.

6. Conclusions

A tritium transport study in non-isothermal conditions has been performed in the HCLL breeder unit and in the WCLL single cell. Results have shown that the inventories of tritium in the lead-lithium and in the Eurofer are almost the same, whereas tritium losses are higher in the WCLL. The time needed to reach the equilibrium condition are in the order of the hour in the HCLL, whilst in the WCLL the equilibrium is reached in less than 20 minutes, with the exception of the hSPs.

References

[1] S. Malang, et al., *An example pathway to a fusion power plant system based on lead-lithium breeder: Comparison of the dual-coolant lead-lithium (DCLL) blanket with the helium-cooled lead-lithium (HCLL) concept as initial step*, Fusion Engineering and Design 84 (2009), 2145-2157.

[2] L. Candido, et al., *Tritium transport in HCLL and WCLL DEMO blankets*, Fusion Engineering and Design 109-111, (2016) 248-254.

[3] U. Fischer, et al., *Neutronics requirements for a DEMO fusion power plant*, Fusion Engineering and Design 98-99 (2015) 2134-2137.

[4] H. Zhang, A. Ying, M. Abdou, *Quantification of dominating factors in tritium permeation in PbLi blankets*, Fusion Science and Technology 68 (2015) 362-367.

[5] C. Moreno, *Preliminary system modeling for WCLL*, Final Report on Deliverable, No.: 2MKYST, 2015.

[6] J. Fradera, *Development and numerical implementation of tritium and helium transport models in liquid metals breeders for nuclear fusion technology applications*, PhD Thesis, 2011.

[7] P. Zhao, W. Yang, Y. Li, Z. Ge, X. Nie, Z. Gao, *Tritium transport analysis for CFETR WCSB blanket*, Fusion Engineering and Design 114 (2017), 26-32.

[8] L. Pan, H. Chen, Q. Zeng, *Tritium transport analysis of HCPB blanket for CFETR*, Fusion Engineering and Design 113 (2016), 82-86.

[9] F. Franza, L.V. Boccaccini, A. Ciampichetti, M. Zucchetti, *Tritium transport analysis in HCPB DEMO blanket with the FUS-TPC code*, Fusion Engineering and Design 88 (2013), 2444-2447.

[10] L. Batet, E. Mas de les Valls, L.A. Sedano, *Mathematical models for tritium permeation analysis in liquid metal flows with helium bubbles*, Fusion Engineering and Design 89 (2014), 1158-1162.

[11] D. Maisonnier, et al., *DEMO and fusion power plant conceptual studies in Europe*, Fusion Engineering and Design 81 (8-14) (2006) 1123-1130.

[12] M. Utili, M. Zucchetti, L. Candido, R. Testoni, *Development of blanket T transport models at BU level for HCLL*, Final Report on Deliverable, No. BB-6.2.3-T001-D002, 2017.

[13] J. Aubert, et al., *Integration for HCLL/DDD 2015 for HCLL (update of DDD 2014)*, Final Report on Deliverable DDD 2015, No. BB-2.1.2-T004-D001, 2016.

[14] A Venturini and D. Martelli, *Literature review of PbLi alloys properties*, Technical report, LM-D-R-262, 2017.

[15] F. Tavassoli, *Fusion Demo Interim Structural Design Criteria (DISDC) - Appendix A Material Design Limit Data A3.S18E Eurofer Steel*, DMN Technical Report DMN/DIR/NT/2004-02/A - TW4-TTMS-005-D01, 2004.

[16] K. Mergia, N. Boukos, *Structural, thermal, electrical and magnetic properties of Eurofer 97 steel*, Journal of Nuclear Materials 373 (2008), 1-8.

[17] S. Chapman, T. G. Cowling, *The mathematical theory of non-uniform gases*, Third Edition, Cambridge Mathematical Library, 1970.

[18] F. Reiter, *Analysis of Simultaneous H and D Permeation through Lithium-Lead*, Fusion Engineering and Design 14 (1991), 207-211.

[19] A. Del Nevo, E. Martelli, M. Oron-Carl, *Integration for WCLL in 2015/DDD 2015 for WCLL (update of DDD 2014)*, Final Report on Deliverable Design Description Document 2015 for WCLL (update of DDD 2014), no. BB-3.1.2-T004-D001, 2016.

[20] C. R. Wilke, and P. Chang, *Correlation of diffusion coefficients in dilute solutions*, AIChE Journal 1 (1955) 264-270.

[21] A. H. Harvey, *Semiempirical correlation for Henry's constants over large temperature ranges*, AIChE Journal 42 (1996), 1491-1494.